International Journal of Agriculture and Biosciences 2026 15(4): 1760-1771.
https://doi.org/10.47278/journal.ijab/2026.082

RESEARCH ARTICLE
eISSN: 2306-3599; pISSN: 2305-6622

Green Synthesis of Silver Nanoparticles using *Prosopis juliflora* (Sw.) DC. Leaves Extract and its Effect on Plant Pathogenic Fungi

Firas M. Abu El Samen [1]*, Oraib K. Al Momani [1], Ayat A. Bozeya [2] and Mohammad M. Al-Gharaibeh [1]

[1]Department of Plant Production Sciences, Faculty of Agriculture, Jordan University of Science and Technology, Irbid, Jordan, 22110
[2]Institute of Nanotechnology, Jordan University of Science and Technology, Irbid, Jordan, 22110
*Corresponding author: hiasat@just.edu.jo

ABSTRACT

The increasing demand for eco-friendly antifungal agents has driven interest in green nanotechnology. In this study, we report a novel, environmentally benign synthesis of silver nanoparticles (AgNPs) using *Prosopis juliflora* leaf extracts, a plant rich in phenols, antioxidants, alkaloids, and flavonoids. AgNPs were formed by dropwise addition of the extract to a silver nitrate ($AgNO_3$) solution, indicated by a color change and confirmed by UV–Visible spectroscopy with a characteristic absorption peak at ~432 nm. Optimization revealed that 25 mL of extract added to 100 mL of 0.01 M $AgNO_3$ at 25 °C yielded highly dispersed AgNPs with 99.3% conversion efficiency. Transmission Electron Microscopy (TEM) showed spherical nanoparticles sized 2–37 nm, and zeta potential analysis indicated good colloidal stability (–23.4 mV). The biosynthesized AgNPs exhibited potent antifungal activity, inhibiting 65–80% of radial mycelial growth in *Fusarium oxysporum*, *Alternaria solani*, *Rhizoctonia solani*, and *Sclerotinia sclerotiorum* at 250–1000 ppm. This work demonstrates, for the first time, the integration of *P. juliflora* bioactives with silver nanoparticles to create a green, sustainable, and highly effective antifungal agent, which has potential applications in agriculture as a natural fungicide to protect crops from phytopathogenic fungi.

Keywords: *Fusarium oxysporum*, *Alternaria solani*, *Rhizoctonia solani*, *Sclerotinia sclerotiorum*, plant pathogens, Fungi.

Article History
Article # 26-046
Received: 16-Jan-26
Revised: 27-Feb-26
Accepted: 07-Mar-26
Online First: 29-Mar-26

INTRODUCTION

Nanotechnology is one of the most active research fields of modern material sciences. Recently, the nanotechnology approach has become of interest in many research areas, including agriculture. This technology employs nano-sized particles with diameters ranging from 1-100 nm and possessing a variety of distinct physical, biological, and chemical properties (Vanlalveni et al., 2021). In agriculture, nanotechnology can be utilized in many applications, including the synthesis of nano-sized pesticides, fertilizers, and growth-promoting compounds (Tahira Gul et al., 2014).

Recently, metal nanoparticles have attracted great scientific interest due to their unique physical and chemical properties. Because of their unusual antimicrobial inhibitory effects, silver nanoparticles (AgNPs) have received great interest among other metal nanoparticles (Roy et al., 2019). Silver is known to attack a broad range of biological processes in microorganisms, including the alteration of cell membrane structure and functions (Dwivedi & Gopal, 2010; Nabikhan et al., 2010). Silver also inhibits the expression of proteins associated with adenosine triphosphate production (Yamanaka et al., 2005), although the specific antimicrobial mechanisms of silver are still not completely understood.

Silver nanoparticles have been suggested in recent studies as an alternative to currently used fungicides. Despite the widespread use of conventional chemical fungicides, their long-term application has led to multiple limitations, including toxicity to non-target organisms, accumulation in soil and water, and harmful impacts on pollinators and beneficial microbes (Yin et al., 2023). Continued use of fungicides with the same modes of

Cite this Article as: Abu El Samen, FM., Al Momani, OK., Bozeya AA and Al-Gharaibeh, MM, 2026. Green synthesis of silver nanoparticles using *Prosopis juliflora* (Sw.) DC. leaves extract and its effect on plant pathogenic fungi. International Journal of Agriculture and Biosciences 15(4): 1760-1771. https://doi.org/10.47278/journal.ijab/2026.082

A Publication of Unique Scientific Publishers

action can lead to the development of fungicide resistance, which has emerged in various plant pathogens and is a serious threat to effective crop protection. Recent studies have highlighted that excessive reliance on these fungicides accelerates the emergence of resistant phytopathogenic fungal strains, making disease control increasingly challenging (Yin et al., 2023). In addition, the extensive environmental footprint associated with these chemicals, ranging from soil degradation to contamination of groundwater, emphasizes the need for safer, more sustainable disease management strategies in agriculture (Kannan et al., 2023; Dávila Costa & Romero, 2025).

Some studies suggested that AgNPs provide comparable efficacy levels compared to conventional fungicides with less likelihood for the development of resistance in target organisms (Kah et al., 2018; Malandrakis et al., 2020). Due to their multi-site action in microbes, compared to the site-specific mode of action of modern systemic fungicides, silver nano-sized materials should be investigated as a more durable and less toxic alternative to currently used fungicides (Park et al., 2006; Kah et al., 2018).

Silver nanoparticles can be synthesized by several physical, chemical, and biological methods (Tahira Gul et al., 2014). The use of plants for nanoparticles synthesis is an exciting possibility that is relatively unexplored and underexploited (Vanlalveni et al., 2021). Green nanotechnology has emerged as a crucial component of sustainable agriculture, offering eco-friendly tools to manage plant diseases while reducing dependence on chemically intensive inputs. With growing concerns over environmental degradation, soil contamination, and biodiversity loss associated with conventional agrochemicals, the development of biologically synthesized nanoparticles, particularly silver nanoparticles (AgNPs), has gained significant attention as a sustainable alternative. Recent studies emphasize that nanotechnology enables precise delivery, enhanced stability, and improved bioactivity of active compounds, making it a promising avenue for modern pest and disease management in agricultural systems. Moreover, plant-mediated AgNPs synthesis integrates naturally occurring phytochemicals as reducing and stabilizing agents, providing a green, cost-effective, and scalable strategy aligned with sustainable agricultural principles (Pan et al., 2022; Thakur et al., 2025).

The green methods of nanoparticles synthesis using plants and microorganisms are low-cost, fast, efficient, and generally lead to the formation of crystalline nanoparticles with a variety of shapes with sizes between 1 and 100 nm (Thakur et al., 2025). These features mainly depend on the process parameters, such as the nature of plant extract and the relative concentrations of the extract and metal salts reacting, pH, temperature, and time of reaction, as well as the rate of mixing of plant extract and metal salts (Thakur et al., 2025).

Green-synthesized AgNPs derived from plant extracts have shown significant promise as a novel class of antifungal agents. Plant-mediated AgNPs synthesis has improved physicochemical control over nanoparticle morphology, size, and stability, enabling enhanced biological performance. Recent comprehensive reviews (Vanlalveni et al., 2021; Thakur et al., 2025) report that phytochemicals such as flavonoids, phenolics, and terpenoids play essential roles in nanoparticle formation by acting as natural reducing and capping agents, ultimately influencing antimicrobial efficacy. Furthermore, studies on various medicinal and herbaceous plants demonstrated strong antifungal activity of biosynthesized AgNPs against pathogenic fungi such as *Candida albicans* and Fusarium *spp*., highlighting their potential as environmentally benign alternatives to chemical fungicides (Al-Zoubi, 2025; Eker et al., 2025).

Plant-derived AgNPs exhibit substantial effectiveness against plant pathogenic fungi, making them particularly relevant for crop protection efforts. Recent experimental research has confirmed the potent antifungal activity of plant-mediated AgNPs synthesized from multiple botanical sources, including *Rhizoctonia solani*, *Cladosporium cladosporioides* (Malik et al., 2024), *Ocimum sanctum* (Abdulwahhab et al., 2026) and *Aristolochia bracteolate* (Tyagi et al., 2024), demonstrating strong inhibitory effects against fungal pathogens such as *Aspergillus flavus*, *Fusarium oxysporum*, and *Candida* species. These findings support the broader applicability of plant extract-derived AgNPs as efficient, eco-friendly antifungal agents and underscore the relevance of exploring underutilized species such as *Prosopis juliflora* for green nanoparticle synthesis. Utilizing the rich phytochemical composition of *P. juliflora* leaves may offer a sustainable and potent biotechnological approach to managing plant pathogenic fungi, ultimately contributing to reduced chemical inputs and improved environmental resilience in agricultural systems.

One of the potential applications in which GAgNPs (Green-Silver Nano-Particles) can be utilized is in the management of plant diseases. Since GAgNPs display multiple modes of inhibitory action to microorganisms, they can be utilized to control various plant pathogens in a relatively safer way compared to synthetic fungicides (Tahira Gul et al., 2014). To our knowledge, until now, few studies have provided some evidence of the applicability of GAgNPs for controlling plant diseases (Abd-Elsalam, 2012).

Phytochemical-rich plant extracts such as those from *Ocimum sanctum* (Tulsi) (Abdulwahhab et al., 2026), *Ficus benghalensis* (Din et al., 2025) serve as powerful reducing and stabilizing agents, enabling rapid, eco-friendly nanoparticle formation with controlled size, morphology, and enhanced stability. For example, green-synthesized AgNPs from Tulsi leaves exhibited spherical crystalline structures averaging ~39.6 nm and showed strong synergistic antimicrobial activity when combined with conventional agents (Abdulwahhab et al., 2026). Similarly, *Ficus benghalensis* extract mediated AgNPs (Din et al., 2025) produced thermodynamically stable, ~41.55 nm nanoparticles with significant enzyme inhibitory and in vivo pharmacological activity. Selvam et al. (2026) emphasize that diverse phytochemicals—flavonoids, terpenoids, polyphenols—directly influence nanoparticle nucleation, growth and stability, expanding biomedical and environmental applications.

Prosopis juliflora (Sw.) DC. is a fast-growing, thorny, deciduous shrub, a drought-resistant plant, which belongs to the *Fabaceae* family. This plant is native to central and South America; in Jordan, this plant is considered an invasive alien species (IAS) (Tadros et al., 2020).

The crude extracts of various parts and purified chemical components have been found to possess antimicrobial, insecticidal, and other pharmacological activities (Sharifi-Rad et al., 2019). Therefore, the present work aimed to investigate the green synthesis of silver nanoparticles using *Prosopis juliflora* leaves extracts as a reducing and capping agent (Raja et al., 2012; Arya et al., 2018), as well as to evaluate the antifungal effect of the prepared AgNPs on a group of plant pathogenic fungi (*Fusarium oxysporum*, *Alternaria solani*, *Rhizoctonia solani*, and *Sclerotinia sclerotiorum*).

MATERIALS & METHODS

Preparation of Plant Material

Prosopis juliflora leaves were collected from the Jordan Valley, from seven different locations North of the Dead Sea in Jordan (Fig. 1).

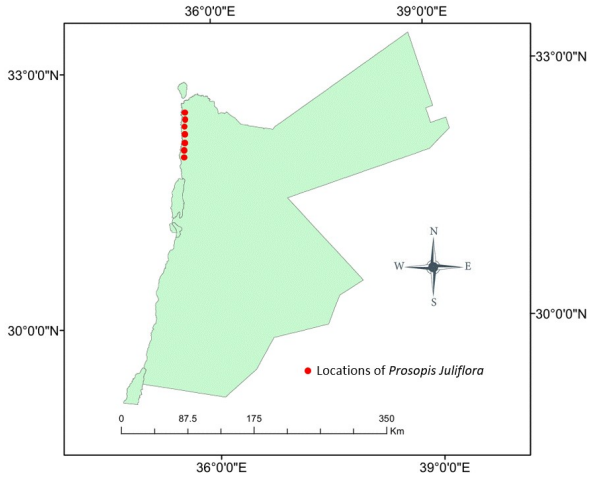

Fig. 1: Sampling locations within the Jordan Valley where *Prosopis juliflora* plant specimens were collected for the synthesis of green silver nanoparticles (GAgNPs).

Leaves were washed with distilled water and were dried at room temperature (25 ± 2℃) for one month. Dried leaves were crushed in an electric grinder (Anwar et al., 2019). Leaf extracts were prepared by taking 20.0 g of *Prosopis juliflora* leaves in a 500 ml Erlenmeyer flask along with 100 ml of distilled water and then boiling the mixture for about 15 min. The *Prosopis juliflora* leaf extracts (PJE) were cooled to room temperature and filtered with Whatman No. 1 filter paper before centrifuging at 5000 rpm for 30 minutes to remove the heavy biomaterials. The PJE was stored at 4°C to be used for further experiments (Raja et al., 2012).

Green Synthesis of Silver Nanoparticles using *Prosopis juliflora* Leaves Extract

To determine the optimum combination of plant leaf extract amount and concentration of (AgNO3) solution to synthesize nano-sized silver particles, [5, 10, 15, 20, and 25 mL] of *Prosopis juliflora* leaf extracts were used (Table 1). In a typical reaction procedure, plant extract (different volumes) was added dropwise to different concentrations of the $AgNO_3$ solutions (1 mM, 2 mM, 0.01 M, and 0.1 M) under continuous stirring at room temperature. Reactions were continuously performed until the color change was observed (Arya et al., 2018). The silver nanoparticle solution was purified by centrifugation at 5000 rpm for 30 minutes and then allowed to dry at room temperature for further use. A total of 20 samples were prepared using different concentration combinations of $AgNO_3$ solutions and plant extract volumes (Table 1).

Table 1: Samples prepared for silver nanoparticles synthesis

$AgNO_3$ concentration	PJE volume (ml)	Sample Number
	5	
	10	
0.01 M	15*	Sample 1
	20*	Sample 2
	25*	Sample 3
	5	
	10	
0.1 M	15*	Sample 4
	20*	Sample 5
	25*	Sample 6
	5	
	10	
1 mM	15	
	20	
	25	
	5	
	10	
2 mM	15	
	20	
	25	

(*) Samples used for silver nanoparticles characterizations.

Physical Characterization of the Synthesized Silver Nanoparticles

The green synthesized silver nanoparticles (GAgNPs) using *Prosopis juliflora* leaves extracts (PJE) as reducing and capping agents were characterized for size, structure, and zeta potential. All synthesized samples of GAgNPs were analyzed using a UV-visible spectroscopy instrument (UV Cary 5000 version 3) to confirm the presence of silver nanoparticles. The shape, size, and zeta potential of the prepared GAgNPs were characterized by transmission electron microscopy (TEM) (Morgani FEi 268), and a zeta potential analyzer (Zeta sizer Nano ZS90, the Malvern Zetasizer UK). The percent of conversion of the synthesized AgNPs was determined using inductively coupled plasma spectrometry (ICP-MS) (iCAP Q- Thermo Scientific).

Fungal Isolates

Four different plant pathogenic fungal isolates were used in this study: *Fusarium oxysporum* f. sp. *cucumerinum*, *Sclerotinia sclerotiorum*, *Alternaria solani*, and *Rhizoctonia solani*. Fungal isolates were purified using the hyphal tip technique and were identified and characterized morphologically and pathologically in the plant pathology lab at Jordan University of Science and Technology (JUST).

Evaluation of the Antifungal Activity of Silver Nanoparticles *in vitro*

The magnitude of radial mycelial growth inhibition of selected fungal isolates (*Fusarium oxysporium*, *Alternaria solani*, *Rhizoctonia solani*, and *Sclerotinia sclerotiorum*) was conducted using different concentrations of *Prosopis juliflora* crude leaves extract (PJE) and different concentrations of synthesized silver nanoparticles (G-AgNPs). Potato dextrose agar (PDA) media plates amended with different concentrations of either PJE or GAgNPs were prepared. Each treatment has a final concentration of PJE or GAgNPs of 50,100, 250, 500, and 1000 ppm (parts per million) (v/v). For comparison purposes, all experiments included an additional treatment using one of the following fungicides used at the manufacturer's recommended application rate: (Revanol® [Hydroxyquinoline sulfate (Quinoline) at 500 ppm]; Bellis® [25.2% Boscald and 12.8% w/w Pyraclostrobin] at 700 ppm; SCORE 250 EC® [Difenoconazole] at 500 ppm; and Tachigaren ® [hymexazol] at 1500 ppm.). Each Petri plate received 20 ml of the amended PDA medium (Raghavendra et al., 2009). The relative growth reduction (inhibition) for each PJE and GAgNPs concentration was calculated after 7 days using equation (1).

$$\text{Percentage of radial mycelium growth inhibition} = 1 - \frac{\text{diameter of the colony on the amended plate}}{\text{diameter of the colony on the control plate}} * 100 \quad (1)$$

Statistical Analysis

In all experiments, values of the mean relative inhibition of radial mycelial growth of different fungal isolates were subjected to analysis of variance (ANOVA), and means were compared by the least significant difference (LSD) test ($P \leq 0.05$). All data were analyzed with JMP software (version 14; SAS Institute Inc.). Levene's test for equality of variances was used to determine if data from different runs of the experiment could be pooled and analyzed together. Results from different runs of the same experiment were pooled together and analyzed only if the homogeneity of variances test indicated no significant difference. Levene's test was conducted using the statistical program Minitab version 19 (Minitab, LLC, Pennsylvania, USA).

RESULTS

Green Synthesis of Silver Nanoparticles using *P. juliflora* Leaves Extract

Depending on the color change when 100 mL of AgNO3 (2 mM, 1 mM, 0.1 M, and 0.01 M) was combined with 5-25 mL of the plant extract, the color change occurred only at 0.1 M and 0.01M. No change in color occurred at 1 mM and 2.0 mM of AgNO3 with 5 - 25 mL of plant extract added. Upon addition of different volumes (15–25 mL) of PJE to 100 mL of aqueous silver nitrate solution at the two optimum concentrations (0.1 M and 0.01 M) (Table 1), the color of the solution changed from faint light to yellowish-brown and finally to the colloidal brown, indicating formation of silver nanoparticles. Silver nanoparticles synthesized at different volumes of JPE (15-25 mL) using 0.01M and 0.1M of silver nitrate were analyzed by inductively coupled plasma mass spectrometry (ICP-MS); the conversion percentages are presented in Table 2. The conversion of Ag+ ions to AgNPs was calculated using equation (2).

$$\frac{Total\ Ag + concentration\ (mg/l) - The\ calculated\ Ag\ concentration\ (mg/l)}{Total\ Ag + concentration\ (mg/l)} * 100\% \quad (2)$$

The ICP-MS results indicated that the conversion factor of Ag+ ions to AgNPs using PJE was at least 97% using 100 mL of 0.01 M AgNO3 with 20 mL from *P. juliflora* extracts (Table 2). Results demonstrated that the best combination of aqueous extract of *P. juliflora* and AgNO3 aqueous solution was achieved using 25 mL of PJE and 100 mL of 0.1 M $AgNO_3$.

Physical Characterization of the GAgNPs

UV– visible spectroscopy was used to confirm the reduction of Ag^+ ions into AgNPs by scanning the reaction mixture after tenfold dilution in the range of wavelengths between 350 and 500 nm. The maximum absorption peak was observed at around 432 nm (Fig. 2), indicating the presence of the GAgNPs, with a size less than 50 nm. The broad peak indicating a heterogeneous size distribution of AgNPs was further confirmed by the TEM and Zeta potential results.

The structure, size, and zeta potential of the prepared GAgNPs were characterized by TEM and a Zeta potential analyzer. The TEM micrograph of the synthesized GAgNPs is shown in Fig. 3. It was observed that most of the GAgNPs shown in the micrograph are spherical in shape for both concentrations of 0.01 M and 0.1 M of AgNO3, with a size range of 2-37 nm. The particle size histogram determined from the TEM images of the nanoparticles indicates that particles are distributed in the range of 2-37 nm with a maximum at 10 nm (Fig. 3).

Table 2: Inductively coupled plasma analysis and calculated conversion percentage of Ag^+ to AgNPs for different preparations of GAgNPs utilizing different combinations of $AgNO_3$ solution concentration and different volumes of PJE

Sample	$AgNO_3$ concentration (M)	AgNO3 Concentration (mg\l)	*Prosopis juliflora* (PJE) volume (ml)	ICP-MS results (mg/l)	Ag+ to AgNPs conversion %
Sample 1	0.01	1079	15	9.359085	99.1%
Sample 2	0.01	1079	20	24.22496	97.7%
Sample 3	0.01	1079	25	6.954622	99.3%
Sample 4	0.1	10789	15	63.43149	99.4%
Sample 5	0.1	10789	20	155.3575	98.5%
Sample 6	0.1	10789	25	45.23956	99.5%

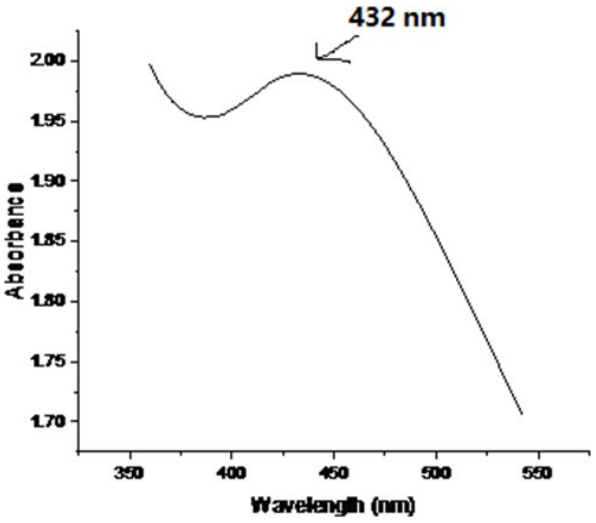

Fig. 2: UV- visible spectra of GAgNPs, maximum absorption peak around 432 nm.

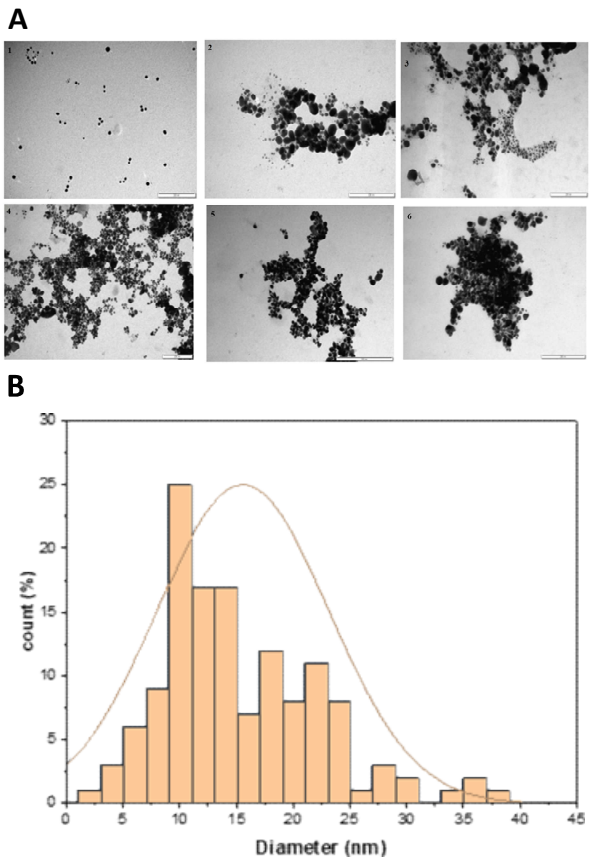

Fig. 3: (A) TEM image for GAgNPs, 1: Sample 1 (0.01 M $AgNO_3$ 15 ml PJE), 2: Sample 2 (0.01 M $AgNO_3$ 20 ml PJE), 3: Sample3 (0.01 M $AgNO_3$ 25 ml PJE), 4: Sample 4 (0.1 M $AgNO_3$ 15 ml PJE), 5: Sample 5 (0.1 M $AgNO_3$ 20 ml PJE), 6: Sample 6 (0.1 M $AgNO_3$ 25 ml PJE). (B) Particle size distribution of GAgNPs.

The Zeta potential (electrokinetic potential) of the synthesized silver nanoparticles ranged from -8.4 to -23.3-millivolts (mV) (Table 3). Sample 3 demonstrated the most negative value (-23.4 mV), suggesting the most stable sample. This sample was synthesized using 100 ml of 0.01M $AgNO_3$ and 25 ml of PJE. This sample was chosen for the anti-fungal activity experiments. Zeta potential measurements demonstrated that the prepared AgNPs were more negative when a 0.01 M concentration of silver nitrate was used (-16.4 mV, -19.6 mV, and -23.4 mV). Overall, the results of the Zeta potential value for GAgNPs indicated the stability of the synthesized nanoparticles (Table 3).

Table 3: The zeta potential of the GAgNPs

Sample	AgNO3 concentration (M)	*Prosopis juliflora* (PJE) volume (ml)	Zeta Potential (ζ) (mV)
Sample 1	0.01	15	-16.4
Sample 2	0.01	20	-19.6
Sample 3	0.01	25	-23.4
Sample 4	0.1	15	-8.4
Sample 5	0.1	20	-12.6
Sample 6	0.1	25	-9.18

Evaluation of the Antifungal Activity of PJE and GAgNPs *in vitro*

In vitro Inhibition of *Alternaria solani* using PJE and GAgNPs

Levene's test for homogeneity of variances indicated that the variance among separate trials was not homogeneous (P>0.5); thus, data of mean percent mycelium growth inhibition from the two runs of the experiment were analyzed and presented separately. In both experimental runs, the highest level of *in vitro* inhibition of radial mycelia growth of *A. solani* was achieved with the fungicide Score® treatment compared to all other levels of PJE and GAgNPs. The mean percent inhibition of the fungicide score was 100% (Fig. 4).

In the first experimental run, the mean percent radial mycelial growth inhibition (% RMGI) achieved with GAgNPs was significantly higher than that of PJE at all concentrations except at 50 ppm, where no significant difference in the level of inhibition was observed. Both treatments, PJE and GAgNPs, resulted in high levels of inhibitory effects; GAgNPs treatments were more potent than PJE. The mean percent inhibition at 1000 ppm was 72% and 79% for PJE and GAgNPs, respectively (Fig. 4-A). At 500 ppm, the mean percent inhibition was 47.5% and 74% for PJE and GAgNPs, respectively (Fig. 4-A). Four folds' increase in mean percent inhibition was observed with 250 ppm of GAgNPs treatment over the same concentration of PJE treatment (Fig. 4-A). Similarly, two folds' increase in inhibition efficacy was observed with 100 ppm concentration of GAgNPs compared to the same concentration of PJE. These results demonstrate that increased efficacy of GAgNPs over PJE can be observed at lower concentrations of the preparations (100-250 ppm) rather than at higher concentrations (Fig. 4).

In the second experimental run (Fig. 4-B), similar trends in mean percent inhibition were observed with different concentrations of GAgNPs and PJE treatments. At all concentrations, except the 500 ppm treatments, there were significant differences between the matching concentrations of GAgNPs and PJE treatments (Fig. 4-B). The greatest difference between the mean percent inhibition of GAgNPs and PJE treatments occurred at 50 ppm and 100 ppm (Fig. 4-B). At 50 ppm concentration, the mean percent inhibition was 39% and 65.8% for PJE and GAgNPs treatments, respectively (Fig. 4-B). At 100 ppm concentration, the mean percent inhibition was 53.1% and 73.9% for PJE and GAgNPs treatments, respectively (Fig. 4-B).

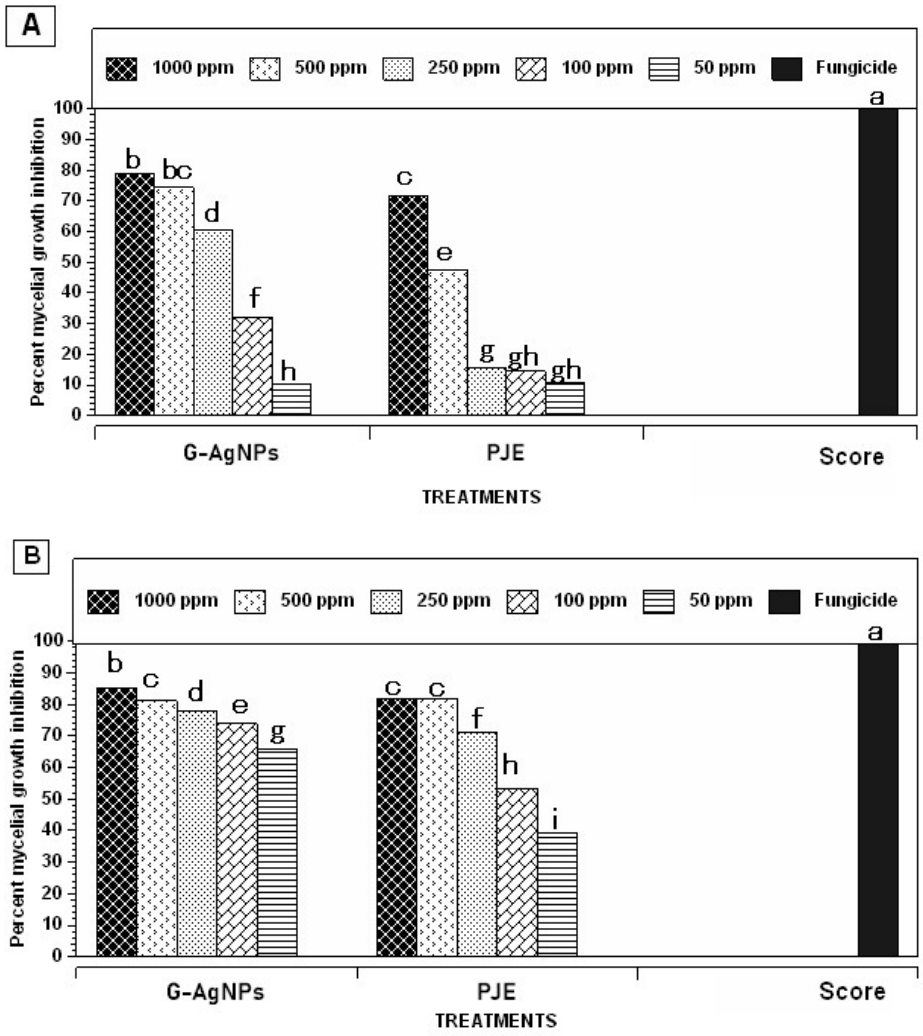

Fig. 4: Mean percentage radial mycelial growth inhibition (% RMGI) of *A. solani* isolate at different concentrations (50 ppm, 100 ppm, 250 ppm, 500 ppm, and 1000 ppm) of G–AgNPs, ethanol extract of *P. juliflora* (PJE), and the fungicide Score (difenoconazole) at 500 ppm. Experiment was repeated twice (A & B), means comparison was conducted using student's t-test at P = 0.05. Least significant differences (LSD) A= 4.732, B= 2.430. Means followed by the same letter (s) are not significantly different.

In vitro Inhibition of *F. oxysporum* f. sp. *cucumerinum* using PJE and GAgNPs

Levene's test for homogeneity of variances indicated that the variance among separate trials was homogeneous ($P<0.05$); thus, data of mean percent mycelium growth inhibition from the two runs of the experiment were pooled and analyzed together. The highest level of *in vitro* inhibition of radial mycelia growth of *F. oxysporum* f. sp. *cucumerinum* was achieved with the fungicide Tachigaren® treatment compared to all other levels of PJE and GAgNPs. The mean percent inhibition of the fungicide Tachigaren® was 100% (Fig. 5). In all treatments [different concentrations of PJE and GAgNPs], there were significant differences in mean percent inhibition of this isolate among the different concentrations of each material (PJE and GAgNPs). The highest level of inhibition was achieved with a 1000 ppm concentration of both PJE and GAgNPs, with 77.1% and 82.9% mean percent inhibition. At all concentrations used, the efficacy of inhibition of mycelial growth was higher with GAgNPs compared to PJE treatments (Fig. 5). The inhibition rate increased gradually by increasing the concentration of each material, but even with a concentration as low as 50 ppm, GAgNPs' mean percent inhibition rate (44%) was higher than that of PJE (34.2 %) (Fig. 5).

In vitro Inhibition of *Sclerotinia sclerotiorum* using PJE and GAgNPs

Levene's test for homogeneity of variances indicated that the variance among separate trials was homogeneous ($P<0.05$), thus data of mean percent mycelium growth inhibition from the two runs of the experiment were pooled and analyzed together.

The highest level of *S. sclerotiorum in vitro* inhibition of radial mycelia growth was achieved with the fungicide Bellis® treatment compared to all other levels of PJE and GAgNPs. The mean percent inhibition of the fungicide Bellis® was 100% (Fig. 6). At high concentrations of both PJE and GAgNPs (1000 ppm and 500 ppm), the difference in the mean percent inhibition was not large. Although at 1000 ppm concentration, the mean percent inhibition was significantly higher with PJE treatment compared to GAgNPs, the difference was not large, and it was in the magnitude of 3% difference only. However, there was no significant difference in mean percent inhibition at a 500-ppm concentration. Results demonstrated that significant differences occurred between the two treatments (PJE and GAgNPs) at lower concentrations (250 ppm, 100 ppm, and 50 ppm). At these lower concentrations, large differences in mean percent inhibition were observed, and GAgNPs were superior in inhibition of the mycelial growth of

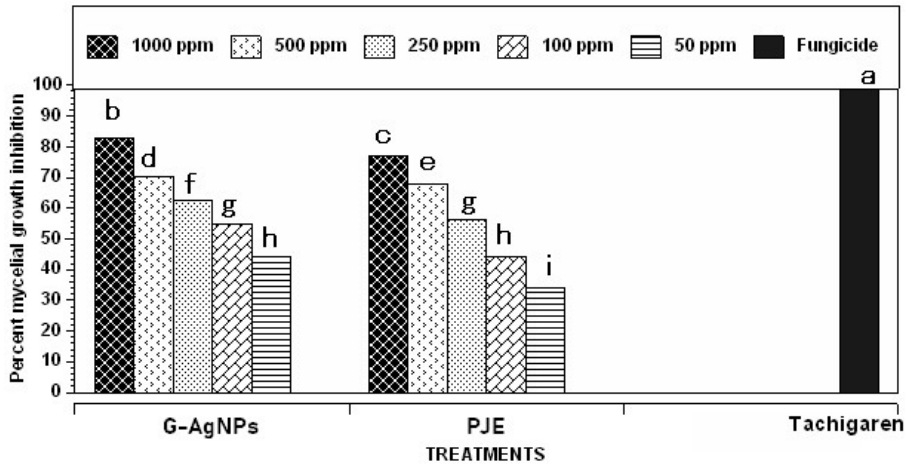

Fig. 5: Mean percentage radial mycelial growth inhibition (% RMGI) of *Fusarium oxysporum* f.sp. *cucumerinum* isolate at different concentrations (50 ppm, 100 ppm, 250 ppm, 500 ppm, and 1000 ppm) of G–AgNPs, ethanol extract of *P. juliflora* (PJE), and the fungicide Tachigaren (Hymexazole) at 1500ppm. Means comparison was conducted using student's t-test at p = 0.05. Least significant differences (LSD) = 2.350. Means followed by the same letter (s) are not significantly different.

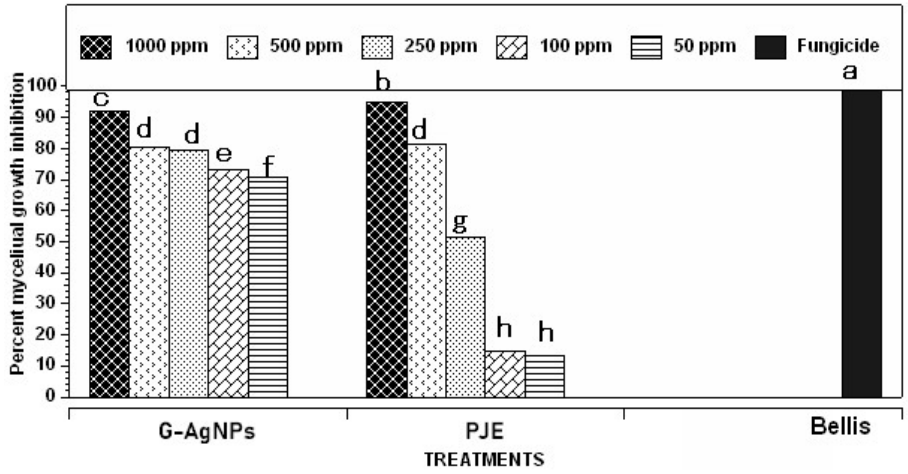

Fig. 6: Mean percentage radial mycelial growth inhibition (%RMGI) of *S. sclerotiorum* isolate at different concentrations (50 ppm, 100 ppm, 250 ppm, 500 ppm, and 1000 ppm) of GAgNPs, ethanol extract of *P. juliflora* (PJE) and fungicide Bellis (Boscalid + Pyraclostrobin) at 700 ppm. Means comparison was conducted using student's t-test at P=0.05. Least significant difference (LSD) = 2.629. Means followed by the same letter (s) are not significantly different.

S. sclerotiorum isolate (Fig. 6). Mean percent inhibition at 250 ppm were 51.2% and 79.2% for PJE and GAgNPs, respectively. At 100 ppm and 50 ppm concentrations, around a 5-fold increase in mycelial growth inhibition was observed with GAgNPs compared to PJE (Fig. 6).

In vitro Inhibition of *Rhizoctonia solani* using PJE and GAgNPs

Levene's test for homogeneity of variances indicated that the variance among separate trials was not homogeneous (P>0.05); thus data of mean percent mycelium growth inhibition from the two runs of the experiment were analyzed and presented separately. In both experimental runs, the highest level of *in vitro* inhibition of radial mycelia growth of *R. solani* isolate was achieved with the fungicide Revanol® treatment compared to all other levels of PJE and GAgNPs. The mean percent inhibition of the fungicide Revanol® was 100% (Fig. 7).

In the first experimental run (Fig. 7A), significant differences in mean percent inhibition of mycelial growth occurred at the high concentration treatments (1000 ppm, 500 ppm, and 250 ppm). At all these concentrations, GAgNPs treatments were superior to PJE treatments. At 1000 ppm concentration, the mean percent inhibition of mycelial growth was 75.8% and 90.9% for PJE and GAgNPs, respectively. Around 2-folds increase in inhibition was achieved with GAgNPs compared to PJE at 250 ppm concentration (Fig. 7A). At 100 ppm and 50 ppm concentrations, the mean percent inhibition was relatively low (less than 20%), and no significant differences in mean percent inhibition were observed between PJE and GAgNPs treatments (Fig. 7A).

In the second experimental run, no significant differences in mean percent mycelial growth inhibition were observed between the two materials (PJE and GAgNPs) at all concentrations (Fig. 7B). The highest mean percent inhibition (80%) was achieved with 1000 ppm of GAgNPs, which was not significantly different from the inhibition achieved with the same concentration of PJE (70.4%) (Fig. 7B). Overall, values of mean percent inhibition were a little bit lower than those observed in the first trial for the higher concentrations (1000 ppm, 500 ppm) of both materials, but higher at the lower concentrations (100 ppm and 50 ppm) (Fig. 7B).

DISCUSSION

Overall, the results indicated that the conversion factor of Ag^{+} ions to AgNPs using PJE was above 97%, which indicates the effectiveness of using *P. juliflora* for the synthesis of silver nanoparticles. The combination of *P. juliflora* extract and AgNO3 at a 1:4 ratio, specifically using 25 ml of PJE and 100 ml of 0.1 M AgNO3, was the most

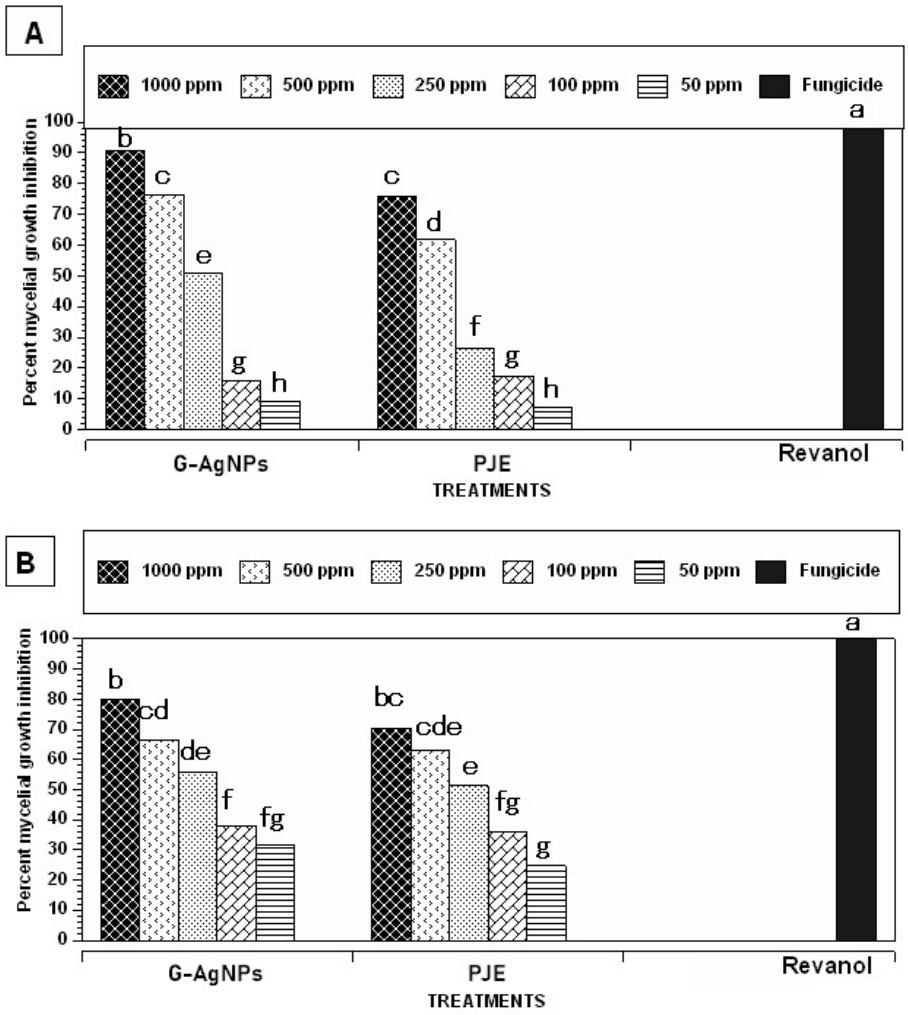

Fig. 7: Mean percentage radial mycelial growth inhibition (% RMGI) of *R. solani* isolate at different concentrations (50 ppm, 100 ppm, 250 ppm, 500 ppm, and 1000 ppm) of G–AgNPs, ethanol extract of *P. juliflora* (PJE), and the fungicide Revanol (sulphate hydroxyquinol) at 500ppm. Experiment was repeated twice (A-B). Means comparison was conducted using student's t-test at p = 0.05. Least significant differences (LSD) A= 5.427, B= 13.105. Means followed by the same letter (s) are not significantly different.

effective condition for synthesizing silver nanoparticles with a conversion factor of 99%. This 1:4 ratio was reported by other researchers as the best combination of plant extracts with $AgNO_3$ solution (Ansari et al., 2023). Other reports indicate that the optimum ratio was (1:5) (Anwar et al., 2019). The physical characterization of the synthesized GAgNPs is essential to understand their properties and suitability for various applications. In this study, multiple techniques were employed to characterize the GAgNPs, including UV-visible spectroscopy, transmission electron microscopy (TEM), and zeta potential analysis.

UV-visible spectroscopy is a widely used technique to confirm the formation of nanoparticles and assess their optical properties. In our study, UV-visible spectroscopy was employed to analyze the absorption spectra of the GAgNPs. The recorded spectrum revealed a prominent absorption peak at approximately 432 nm (Fig. 2). This observation is consistent with the presence of GAgNPs, and the peak's position suggests that the synthesized nanoparticles have a size less than 50 nm. It's noteworthy that similar studies by other researchers have reported absorption peaks around 420 nm and 440 nm (Malini et al., 2020). The shift in the absorption peak is usually indicative of a larger particle size, and a broader peak for smaller size particles (Nabikhan et al., 2010). These findings confirm the successful reduction of Ag+ ions into GAgNPs and their size characteristics.

To gain insight into the structure and size distribution of the GAgNPs, Transmission Electron Microscopy (TEM) analysis was performed. TEM showed spherical nanoparticles sized 2–37 nm. The results of this analysis are consistent with the findings of other researchers who reported similar particle size ranges in their studies. One study reported that the particle size was in the range of (10-50 nm) (Arya et al., 2018). Other studies showed that the size ranged between 35-60 nm (Rai & Ingle, 2012) and 85 nm (Malini et al., 2020). Particularly, nanoparticles within this size range are desirable for various applications due to their unique properties and potential effectiveness.

Zeta potential, which represents the electrokinetic potential of nanoparticles, is a crucial parameter that influences the stability and behavior of colloidal suspensions. Particle-to-particle interaction is a crucial element in determining the characteristics of colloidal suspensions. One of the most important forces is electrokinetic repulsion. It is produced by a charge which is almost always found on the surfaces of the particles in liquids. If their surface charge is relatively high, then adjacent colloids will repel each other and will tend to maintain their individuality. As a result, highly charged colloids tend to remain discrete and in suspension. On the other hand, a colloid with little or no charge has little

resistance to the natural tendency for fine particles to gather into aggregates. Small clumps will form and, in turn, aggregate into larger flocs which settle quickly or form an interconnected matrix. In this study, the range of Z-potential was -8.4mV to -23.4 Mv. A similar result was reported by Arya et al., 2018. In another study (Mfon & Al Amri, 2023), reported a Zeta potential of – 15.03 mV to – 20.3 mV for silver nanoparticles prepared from *Ocimum gratissimum* plant extracts, while that of GAgNPs prepared from *Vernonia amygdalina* leaf extracts was from – 23.41 mV to – 27.23 mV. They reported that this range of zeta potentials indicates some instability and shows that the nanoparticles were on the threshold of agglomeration and could support stabilization but may not favor protein absorption from drugs (Mfon & Al Amri, 2023).

In this study, as indicated from the TEM images, as the concentration of the GAgNPs increases, the agglomeration of the AgNPs is expected to occur. The higher the agglomeration, the lower the relative movement of the nanoparticles to the solvent and hence the lower the zeta potential values. This indicates that the AgNPs concentration resulting from the 0.01 M AgNO3 to 25 ml is the optimum value to ensure the free movement of the NPs and hence the optimum effects (Vanlalveni et al., 2021).

In this study, the successful synthesis of AgNPs is evidenced by a surface plasmon resonance band around 400–450 nm (peak around 432nm) in UV–Visible spectra (Rai et al., 2009). UV-visible spectroscopy is a commonly used analytical technique to examine the formation of AgNPs. When interacting with an electromagnetic field, the electrons present in the outermost orbital of metal nanoparticles oscillate in resonance with certain wavelengths to exhibit a phenomenon called surface plasmon resonance (SPR). The excitation of SPR is responsible for the formation of color and absorbance in a colloidal solution of AgNPs. The SPR peaks at around 435 nm are usually taken to confirm the reduction of silver nitrate into AgNPs (Vanlalveni et al., 2018). In general, spherical NPs exhibit only a single SPR band in the absorbance spectra as seen in this study, whereas two or more SPR bands were observed for anisotropic particles depending on the shape (Vanlalveni et al., 2021).

In this research, crude leaf extracts of *P. juliflora* were highly effective in inhibiting the plant pathogenic fungal isolates tested in this study (*Fusarium oxysporum, Alternaria solani, Rhizoctonia solani, and Sclerotinia sclerotiorum*). These findings agree with recent reports that investigated the efficacy of *Prosopis spp*. against fungal and bacterial pathogens (Saleh & Abu-Dieyeh, 2021). Saleh & Abu-Dieyeh (2021) reported that *P. juliflora* leaf ethanolic extract displayed the strongest antibacterial activity. PDA plates with 20 mg/ml *P. juliflora* leaf extract showed 100% inhibition of the growth of *Botrytis cinerea* and *Alternaria alternata*. High percent inhibition of mycelial growth was also shown against *Geotrichum candidum*, *Colletotrichum gloeosporioides,* and *Fusarium oxysporum* (Saleh & Abu-Dieyeh, 2021).

In the current study, the antifungal activity of *P. juliflora*-derived GAgNPs was investigated against four different plant pathogenic fungi *(Fusarium oxysporum* f. sp. *cucumerinum, Alternaria solani, Rhizoctonia solani,* and *Sclerotinia sclerotiorum).* The results demonstrate that GAgNPs were, in most cases, superior to PJE in inhibiting different fungal isolates. These results are consistent with previously published reports, which demonstrated enhanced efficacy of inhibition of GAgNPs over crude plant extracts (Choudhury et al., 2016; Garibo et al., 2020). Recently, Garibo et al. (2020) reported that the antimicrobial activity was enhanced using AgNPs synthesized from an aqueous extract of *L. acapulcensis* due to the combination with their antimicrobial substances present in the extract (Garibo et al., 2020). In addition, Choudhury et al. (2016) reported that the use of medicinal plants in the synthesis of GAgNPs is not only used for size and shape control, but also for providing plant antimicrobial properties to AgNPs (Choudhury et al., 2016; Vanlalveni et al., 2021).

The green synthesis of AgNPs using *Prosopis juliflora* (Sw.) DC. Leaf extracts represent an environmentally friendly and sustainable alternative to conventional synthesis methods (Ahmed et al., 2016; Vanlalveni et al., 2021). The leaf extract of *P. juliflora* contains bioactive phytochemicals that facilitate the reduction of Ag^{+} ions to Ag^{0} nanoparticles (Abbas et al., 2022). These biomolecules also function as capping and stabilizing agents, enhancing nanoparticle stability and preventing agglomeration (Ahmed et al., 2016). GAgNPs synthesized using *P. juliflora* leaf extract have demonstrated enhanced antimicrobial activity probably due to a synergistic effect between silver and plant-derived compounds (Abbas et al., 2022; Rai et al., 2009). Compared with chemical synthesis routes, green synthesis avoids hazardous reagents and improves environmental compatibility (Ahmed et al., 2016). Thus, *Prosopis juliflora* serves as a valuable biological resource for sustainable nanomaterial production (Ahmed et al., 2016).

The antifungal activity of *P. juliflora*–mediated GAgNPs against plant pathogenic fungi such as *Fusarium oxysporum, Alternaria solani, Rhizoctonia solani, and Sclerotinia sclerotiorum* can also be attributed to their small particle size, high surface area, and enhanced reactivity. The mode of action of silver nanoparticles is not fully clear; however, it has been suggested that these particles might attach to and penetrate the cell membrane to kill fungal cells and spores. Although penetration of silver nanoparticles into microbial cell membranes is not completely understood, it has been suggested that it could involve the destruction of membrane integrity (Jo et al., 2009). Further, AgNPs could disrupt fungal cell membranes, increase membrane permeability, and induce structural damage to hyphae and spores, leading to leakage of cellular contents and inhibition of mycelial growth (Kim et al., 2009; Rai et al., 2009). Microscopic observations reported in related studies revealed deformed hyphal structures, reduced spore germination, and abnormal branching in fungi treated with AgNPs synthesized via plant extracts (Jo et al., 2009).

In addition to physical membrane damage, AgNPs generate reactive oxygen species (ROS), which cause

oxidative stress, lipid peroxidation, protein denaturation, and DNA damage in fungal cells, ultimately leading to cell death (Kumar et al., 2018). The presence of bioactive compounds from *P. juliflora* on the surface of GAgNPs may further enhance antifungal efficacy through synergistic effects, as these phytochemicals themselves possess inherent antimicrobial properties (Vanlalveni et al., 2021). This biofunctionalization improves nanoparticle stability and facilitates stronger interactions with fungal cells.

In this research, inhibition of mycelial growth of fungal isolates increased as the concentration of GAgNPs increased; these results agree with recent studies that also demonstrated that the inhibition of mycelial growth increased along with the concentration (Jo et al., 2009; Saleh & Abu-Dieyeh, 2021). This could be due to the high density at which the solution was able to saturate and adhere to fungal hyphae and to deactivate the growth of pathogenic fungi (Jo et al., 2009). In addition, results of different experimental runs suggest that values of mean percent inhibition of mycelial growth might vary from one experimental run to another; however, it also suggests that we can achieve adequate levels of inhibitory effects by using lower concentrations of GAgNPs. Antifungal action of several types of nanoparticles and their combinations has been reported against other plant pathogens such as *Raffaelea spp*., *Bipolaris sorokiniana*, *Magnaporthe grisea*, *Fusarium spp.*, *Phoma spp., Botrytis cinerea*, *Alternaria alternata*, *Alternaria solani*, *Fusarium solani*, *Colletotrichum circinans*, gram-negative and gram-positive bacteria (Abbas et al., 2022; Jo et al., 2009; Kim et al., 2009; Rai & Ingle, 2012; Saleh & Abu-Dieyeh, 2021). Strong inhibition of the fungal pathogen *Sclerotinia sclerotiorum* by AgNPs observed in this study agrees with recent studies that investigated the effect of GAgNPs on this pathogen. Recent studies (El-Ashmony et al., 2022; Singh et al., 2024) documented strong *in vitro* inhibition and even disease suppression *in planta* with biogenic AgNPs. For example, GAgNPs synthesized using *Trichoderma harzianum*(El-Ashmony et al., 2022) suppressed *S. sclerotiorum* and *S. rolfsii* and reduced disease severity in bean/sunflower foliage, consistent with results of this study, which demonstrated 80% radial inhibition at 1000 ppm and significant activity at 250 ppm. Similarly, the inhibition of the fungal pathogen *Rhizoctonia solani,* observed in this study, using GAgNPs was also recently reported by Islam et al. (2024). Islam et al. (2024) demonstrated that GAgNPs significantly inhibited mycelial growth of *Rhizoctonia solani*, and further greenhouse and field experiments validated the antifungal efficacy of GAgNPs against sheath blight disease in rice, exhibiting comparable effectiveness to commercial fungicides (Islam et al., 2024). Similar results of strong inhibition of fungal growth by GAgNPs were also reported recently for the pathogens *Fusarium oxysporum* (Qureshi et al., 2023) and *Alternaria solani* (Khatoon et al., 2024).

Conclusions

In conclusion, the results of this study suggest that *Prosopis juliflora* leaves extract can be used as a reducing and capping agent for the synthesis of silver nanoparticles, which showed a great antifungal inhibitory effect. Findings from the current investigation demonstrated that both crude leaf extract of *P. juliflora* and GAgNPs provided adequate levels of inhibition of fungal isolates tested in this study. Compared to crude leaf extracts, *P. juliflora*–derived GAgNPs exhibit significantly higher antifungal activity at lower concentrations, indicating enhanced bioavailability and potency of silver in its nanoscale form (Rai & Ingle, 2012; Singh et al., 2024). This makes GAgNPs promising candidates for managing plant diseases while reducing reliance on synthetic fungicides. Moreover, their biodegradable nature and reduced environmental toxicity align with sustainable agriculture and integrated pest management strategies. The investigation was carried out using *in vitro* techniques. The efficacy of GAgNPs in plant disease management was not investigated in this study. Future work should investigate the efficacy of GAgNPs from *P. juliflora* in greenhouse and field experiments utilizing different doses and application methods. Overall, the findings support the potential application of *Prosopis juliflora*–mediated GAgNPs as effective antifungal agents in plant disease control. However, further studies are necessary to evaluate their phytotoxicity, long-term environmental impact, and field-level efficacy before large-scale agricultural applications.

DECLARATIONS

Funding: This research was funded by the Deanship of Scientific Research, Jordan University of Science and Technology, Grant no. 225-2019.

Acknowledgement: The authors are grateful to the Deanship of Scientific Research, Jordan University of Science and Technology, for financial support of this research. We acknowledge the critical revision of the manuscript and suggestions provided by Prof. Kholoud Alananabeh from the Department of Plant Protection at the University of Jordan and Prof. Borhan Aldeen Albiss from the Institute of Nanotechnology, Jordan University of Science and Technology.

Conflict of Interest: The authors declare that the research was conducted in the absence of any commercial or financial relationships that could be construed as a potential conflict of interest.

Data Availability: The original contributions presented in the study are included in the article; further inquiries can be directed to the corresponding author.

Ethics Statement: The study does not involve any animals or human experiments, thus not required.

Author's Contribution: Conceptualization, Abu El Samen F.M., Al Momani O and Bozeya A.; Methodology, Abu El Samen F.M., Al Momani O, Al-Gharaibeh and M Bozeya A.; software and statistical analysis, Al Momani O and Abu El Samen F.M; Validation, Abu El Samen F.M., and Al-Gharaibeh M.; Formal Analysis, Abu El Samen F.M. and

Bozeya A.; Investigation, Abu El Samen F.M., Al Momani O and Bozeya A.; Resources, Abu El Samen F.M., and Bozeya A.; data curation, Abu El Samen F.M. and Bozeya A.; Writing—original draft preparation, Abu El Samen F.M., Al Momani O.; Writing—review and editing, Abu El Samen F.M and Al-Gharaibeh M; Visualization, Abu El Samen F.M.; Supervision, Abu El Samen F.M. and Bozeya A.; Project administration, Abu El Samen F.M..; Funding acquisition, Abu El Samen, F.M. All authors have read and agreed to the published version of the manuscript.

Generative AI Statement: The authors declare that no Gen AI/DeepSeek was used in the writing/creation of this manuscript.

Publisher's Note: All claims stated in this article are exclusively those of the authors and do not necessarily represent those of their affiliated organizations or those of the publisher, the editors, and the reviewers. Any product that may be evaluated/assessed in this article or claimed by its manufacturer is not guaranteed or endorsed by the publisher/editors.

REFERENCES

Abbas, A.M., Novak, S.J., Fictor, M., Mostafa, Y.S., Alamri, S.A., Alrumman, S.A., Taher, M.A., Hashem, M., & Khalaphallah, R. (2022). Initial in vitro assessment of the antifungal activity of aqueous extracts from three invasive plant species. *Agriculture, 12*(8), 1152. https://doi.org/10.3390/agriculture12081152

Abd-Elsalam, K.A. (2012). Nanoplatforms for plant pathogenic fungi management. *Fungal Genomics & Biology, 2*(2), e107. https://doi.org/10.4172/2165-8056.1000e107

Abdulwahhab, N.I., Mohamed, E.A., Aljaafari, H.A.S., Mahmood, B.S., Hasoon, B.A., Zghair, Z.M., Sultan, A.J., & Anaee, R.A. (2026). Green-synthesized silver nanoparticles from Tulsi leaf extract: Synergistic antimicrobial activity against bacterial and fungal pathogens. *Journal of Umm Al-Qura University for Applied Sciences, 13*, 768. https://doi.org/10.1007/s43994-026-00315-z

Ahmed, S., Ahmad, M., Swami, B.L., & Ikram, S. (2016). A review on plant extract-mediated synthesis of silver nanoparticles for antimicrobial applications: A green expertise. *Journal of Advanced Research, 7*(1), 17–28. https://doi.org/10.1016/j.jare.2015.02.007

Al-Zoubi, O.M. (2025). Biosynthesis of silver nanoparticles utilizing Yanbu's indigenous medicinal herbs and plants: Antimicrobial activities evaluation. *Journal of Pure and Applied Microbiology, 19*(1), 485–497. https://doi.org/10.22207/JPAM.19.1.39

Ansari, M., Ahmed, S., Abbasi, A., Khan, M.T., Subhan, M., Bukhari, N.A., Hatamleh, A.A., & Abdelsalam, N.R. (2023). Plant-mediated fabrication of silver nanoparticles, process optimization, and impact on tomato plant. *Scientific Reports, 13*(1), 45038. https://doi.org/10.1038/s41598-023-45038-x

Anwar, Y., Fakieh, M.H., Ullah, I., Alkenani, N.A., & Sharif, M.A. (2019). Synthesis of silver nanoparticles using *Prosopis juliflora* extract: Potential antimicrobial and pollutants degradation performance. *Desalination and Water Treatment, 167*, 105–112. https://doi.org/10.5004/dwt.2019.24571

Arya, G., Kumari, R.M., Gupta, N., Kumar, A., Chandra, R., & Nimesh, S. (2018). Green synthesis of silver nanoparticles using *Prosopis juliflora* bark extract: Reaction optimization, antimicrobial and catalytic activities. *Artificial Cells, Nanomedicine, and Biotechnology, 46*(5), 985–993. https://doi.org/10.1080/21691401.2017.1354302

Choudhury, R., Majumder, M., Roy, D.N., Basumallick, S., & Misra, T.K. (2016). Phytotoxicity of Ag nanoparticles prepared by biogenic and chemical methods. *International Nano Letters, 6*(3), 153–159. https://doi.org/10.1007/s40089-016-0181-z

Dávila Costa, J.S., & Romero, C.M. (2025). Nano-biofungicides and bio-nanofungicides: State of the art of innovative tools for controlling resistant phytopathogens. *Biophysica, 5*(2), 15. https://doi.org/10.3390/biophysica5020015

Din, I.U., Ajaj, R., Rauf, A., Ahmad, Z., Muhammad, N., Ali, S., Hemeg, H.A., & Ullah, I. (2025). *Ficus benghalensis* extract mediated green synthesis of silver nanoparticles: Optimization, characterization, computational studies, and its in vitro and in vivo biological potential. *PLOS ONE, 20*, e0326858. https://doi.org/10.1371/journal.pone.0326858

Dwivedi, A.D., & Gopal, K. (2010). Biosynthesis of silver and gold nanoparticles using *Chenopodium album* leaf extract. *Colloids and Surfaces A: Physicochemical and Engineering Aspects, 369*(1–3), 27–33. https://doi.org/10.1016/j.colsurfa.2010.07.020

Eker, F., Akdaşçi, E., Duman, H., Bechelany, M., & Karav, S. (2025). Green synthesis of silver nanoparticles using plant extracts: A comprehensive review of physicochemical properties and multifunctional applications. *International Journal of Molecular Sciences, 26*(13), 6222. https://doi.org/10.3390/ijms26136222

El-Ashmony, R.M.S., Zaghloul, N.S.S., Milošević, M., Mohany, M., Al-Rejaie, S. S., Abdallah, Y., & Galal, A.A. (2022). The biogenically efficient synthesis of silver nanoparticles using the fungus *Trichoderma harzianum* and their antifungal efficacy against *Sclerotinia sclerotiorum* and *Sclerotium rolfsii*. *Journal of Fungi, 8*(6), 597. https://doi.org/10.3390/jof8060597

Garibo, D., Borbón-Nuñez, H.A., de León, J.N.D., García Mendoza, E., Estrada, I., Toledano-Magaña, Y., Tiznado, H., Ovalle-Marroquin, M., Soto-Ramos, A.G., Blanco, A., Rodríguez, J.A., Romo, O.A., Chávez-Almazán, L.A., & Susarrey-Arce, A. (2020). Green synthesis of silver nanoparticles using *Lysiloma acapulcensis* exhibits high antimicrobial activity. *Scientific Reports, 10*(1), 69606. https://doi.org/10.1038/s41598-020-69606-7

Islam, A.K.M.S., Bhuiyan, R., Nihad, S.A.I., Akter, R., Khan, M.A.I., Akter, S., Islam, M.R., Khokon, M.A.R., & Latif, M.A. (2024). Green synthesis and characterization of silver nanoparticles and its efficacy against *Rhizoctonia solani*, a fungus causing sheath blight disease in rice. *PLOS ONE, 19*, e0304817. https://doi.org/10.1371/journal.pone.0304817

Jo, Y.K., Kim, B.H., & Jung, G. (2009). Antifungal activity of silver ions and nanoparticles on phytopathogenic fungi. *Plant Disease, 93*(10), 1037–1043. https://doi.org/10.1094/PDIS-93-10-1037

Kah, M., Kookana, R.S., Gogos, A., & Bucheli, T.D. (2018). A critical evaluation of nanopesticides and nanofertilizers against their conventional analogues. *Nature Nanotechnology, 13*(8), 677–684. https://doi.org/10.1038/s41565-018-0131-1

Kannan, M., Bojan, N., Swaminathan, J., Zicarelli, G., Hemalatha, D., Zhang, Y., Ramesh, M., & Faggio, C. (2023). Nanopesticides in agricultural pest management and their environmental risks: A review. *International Journal of Environmental Science and Technology, 20*, 10507–10532. https://doi.org/10.1007/s13762-023-04795-y

Khatoon, J., Mehmood, A., Khalid, A. ur R., Khan, M.A.R., Ahmad, K.S., Amjad, M.S., Bashir, U., Raffi, M., & Proćków, J. (2024). Green-fabricated silver nanoparticles from *Quercus incana* leaf extract to control the early blight of tomatoes caused by *Alternaria solani*. *BMC Plant Biology, 24*(1), 5008. https://doi.org/10.1186/s12870-024-05008-5

Kim, S.W., Kim, K.S., Lamsal, K., Kim, Y.J., Kim, S.B., Jung, M., Sim, S.J., Kim, H.S., Chang, S.J., Kim, J.K., & Lee, Y.S. (2009). An in vitro study of the antifungal effect of silver nanoparticles on oak wilt pathogen *Raffaelea* sp. *Journal of Microbiology and Biotechnology, 19*(8), 760–764. https://doi.org/10.4014/jmb.0812.649

Kumar, M., Bansal, K., Gondil, V.S., Sharma, S., Jain, D.V.S., Chhibber, S., Sharma, R.K., & Wangoo, N. (2018). Synthesis, characterization, mechanistic studies, and antimicrobial efficacy of biomolecule-capped and pH-modulated silver nanoparticles. *Journal of Molecular Liquids, 249*, 1145–1150. https://doi.org/10.1016/j.molliq.2017.11.143

Malandrakis, A.A., Kavroulakis, N., & Chrysikopoulos, C.V. (2020). Use of silver nanoparticles to counter fungicide resistance in *Monilinia fructicola*. *Science of the Total Environment, 747*, 141287. https://doi.org/10.1016/j.scitotenv.2020.141287

Malik, M.A., Wani, A.H., Bhat, M.Y., Siddiqui, S., Alamri, S.A.M., & Alrumman, S.A. (2024). Fungal-mediated synthesis of silver nanoparticles: A novel strategy for plant disease management. *Frontiers in Microbiology, 15*, 1399331. https://doi.org/10.3389/fmicb.2024.1399331

Malini, S., Vignesh Kumar, S., Hariharan, R., Pon Bharathi, A., Renuka Devi, P., & Hemananthan, E. (2020). Antibacterial, photocatalytic, and biosorption activity of chitosan nanocapsules embedded with *Prosopis juliflora* leaf extract-synthesized silver nanoparticles. *Materials Today: Proceedings, 21*, 828–832. https://doi.org/10.1016/j.matpr.2019.07.587

Mfon, R.E., & Al Amri, Z. (2023). Synthesis, characterisation and zeta potential of silver nanoparticles. *American Journal of Sciences and Engineering Research, 6*, 104–110.

Nabikhan, A., Kandasamy, K., Raj, A., & Alikunhi, N.M. (2010). Synthesis of antimicrobial silver nanoparticles by callus and leaf extracts from

saltmarsh plant, *Sesuvium portulacastrum* L. *Colloids and Surfaces B: Biointerfaces, 79*(2), 488–493. https://doi.org/10.1016/j.colsurfb.2010.05.018

Pan, X., Guo, X., Zhai, T., Zhang, D., Rao, W., Cao, F., & Guan, X. (2022). Nanobiopesticides in sustainable agriculture: Developments, challenges, and perspectives. *Environmental Science: Nano, 10*, 41–61. https://doi.org/10.1039/d2en00605g

Park, H.J., Kim, S.H., Kim, H.J., & Choi, S.H. (2006). A new composition of nanosized silica-silver for control of various plant diseases. *Plant Pathology Journal, 22*(3), 295–302.

Qureshi, A.K., Farooq, U., Shakeel, Q., Ali, S., Ashiq, S., Shahzad, S., Tariq, M., Seleiman, M.F., Jamal, A., Saeed, M.F., & Manachini, B. (2023). The green synthesis of silver nanoparticles from *Avena fatua* extract: Antifungal activity against *Fusarium oxysporum* f. sp. *lycopersici*. *Pathogens, 12*(10), 1247. https://doi.org/10.3390/pathogens12101247

Rai, M., & Ingle, A. (2012). Role of nanotechnology in agriculture with special reference to management of insect pests. *Applied Microbiology and Biotechnology, 94*, 287–293. https://doi.org/10.1007/s00253-012-3969-4

Rai, M., Yadav, A., & Gade, A. (2009). Silver nanoparticles as a new generation of antimicrobials. *Biotechnology Advances, 27*, 76–83. https://doi.org/10.1016/j.biotechadv.2008.09.002

Raja, K., Saravanakumar, A., & Vijayakumar, R. (2012). Efficient synthesis of silver nanoparticles from *Prosopis juliflora* leaf extract and its antimicrobial activity using sewage. *Spectrochimica Acta Part A: Molecular and Biomolecular Spectroscopy, 97*, 490–494. https://doi.org/10.1016/j.saa.2012.06.038

Roy, A., Bulut, O., Some, S., Mandal, A.K., & Yilmaz, M.D. (2019). Green synthesis of silver nanoparticles: Biomolecule–nanoparticle organizations targeting antimicrobial activity. *RSC Advances, 9*, 2673–2702. https://doi.org/10.1039/c8ra08982e

Saleh, I., & Abu-Dieyeh, M.H. (2021). Novel *Prosopis juliflora* leaf ethanolic extract as a natural antimicrobial agent against food-spoiling microorganisms. *Scientific Reports, 11*(1), 86503. https://doi.org/10.1038/s41598-021-86509-3

Selvam, K., Ragu Prasath, A., & Alanazi, A.K. (2026). A review of recent developments in green synthesis of silver nanoparticles: Antioxidant and antibacterial applications. *Microscopy Research and Technique, 89*, 134–147. https://doi.org/10.1002/jemt.70060

Sharifi-Rad, J., Kobarfard, F., Ata, A., Ayatollahi, S.A., Khosravi-Dehaghi, N., Jugran, A.K., Tomas, M., Capanoglu, E., Matthews, K.R., Popović-Djordjević, J., Kostić, A., Kamiloglu, S., Sharopov, F., Choudhary, M.I., & Martins, N. (2019). *Prosopis* plant chemical composition and pharmacological attributes: Targeting clinical studies from preclinical evidence. *Biomolecules, 9*, 777. https://doi.org/10.3390/biom9120777

Singh, J., Kumar, A., Nayal, A.S., Vikal, S., Shukla, G., Singh, A., Singh, A., Goswami, S., Kumar, A., Gautam, Y.K., Verma, Y., Gaurav, S.S., & Pratap, D. (2024). Comprehensive antifungal investigation of green-synthesized silver nanoformulation against four agriculturally significant fungi and its cytotoxic applications. *Scientific Reports, 14*(1), 56619. https://doi.org/10.1038/s41598-024-56619-9

Tadros, M.J., Al-Assaf, A., Othman, Y.A., Makhamreh, Z., & Taifour, H. (2020). Evaluating the effect of *Prosopis juliflora*, an alien invasive species, on land cover change using remote sensing approach. *Sustainability, 12*(15), 887. https://doi.org/10.3390/su12155887

Tahira Gul, H., Saeed, S., Zafar, F., Khan, A., & Manzoor, S.A. (2014). Potential of nanotechnology in agriculture and crop protection: A review. *Applied Sciences and Business Economics, 1*, 23–28.

Thakur, N., Tapwal, A., Kumari, K., Thakur, R.K., Ganesamoorthy, R., & Thirugnanasambandham, K. (2025). Advancements in biogenic nanoparticles synthesis, characterization and its mechanism in disease management. *Bioresource Technology Reports, 31*, 102227. https://doi.org/10.1016/j.biteb.2025.102227

Tyagi, R., Kumari, M., & Singh, S. (2024). Characterisation and synthesis of AgNPs from *Aristolochia bracteolata* leaves. *International Journal of Multidisciplinary Research and Growth Evaluation, 5*(5), 148–154. https://doi.org/10.54660/.ijmrge.2024.5.5.148-154

Vanlalveni, C., Lallianrawna, S., Biswas, A., Selvaraj, M., Changmai, B., & Rokhum, S.L. (2021). Green synthesis of silver nanoparticles using plant extracts and their antimicrobial activities: A review of recent literature. *RSC Advances, 11*, 2804–2837. https://doi.org/10.1039/d0ra09941d

Vanlalveni, C., Rajkumari, K., Biswas, A., Adhikari, P.P., Lalfakzuala, R., & Rokhum, L. (2018). Green synthesis of silver nanoparticles using *Nostoc linckia* and its antimicrobial activity: A novel biological approach. *BioNanoScience, 8*(2), 624–631. https://doi.org/10.1007/s12668-018-0520-9

Yamanaka, M., Hara, K., & Kudo, J. (2005). Bactericidal actions of a silver ion solution on *Escherichia coli*, studied by energy-filtering transmission electron microscopy and proteomic analysis. *Applied and Environmental Microbiology, 71*(11), 7589–7593. https://doi.org/10.1128/AEM.71.11.7589-7593.2005

Yin, Y., Miao, J., Shao, W., Liu, X., Zhao, Y., & Ma, Z. (2023). Fungicide resistance: Progress in understanding mechanism, monitoring, and management. *Phytopathology, 113*, 707–718. https://doi.org/10.1094/PHYTO-10-22-0370-KD